

Seismological Research Letters

This copy is for distribution only by
the authors of the article and their institutions
in accordance with the Open Access Policy of the
Seismological Society of America.

For more information see the publications section
of the SSA website at www.seismosoc.org



THE SEISMOLOGICAL SOCIETY OF AMERICA
400 Evelyn Ave., Suite 201
Albany, CA 94706-1375
(510) 525-5474; FAX (510) 525-7204
www.seismosoc.org

Empirical Estimation of High-Frequency Ground Motion on Hard Rock

by Olga-Joan Ktenidou and Norman A. Abrahamson

ABSTRACT

Site effects for hard-rock sites are typically computed using analytical models for the effect of κ_0 , the high-frequency attenuation parameter. New datasets that are richer in hard-rock recordings allow us to evaluate the scaling for hard-rock sites (e.g., $V_{S30} > 1500$ m/s). The high-frequency response spectra residuals are weakly correlated with κ_0 , in contrast to the strong scaling with κ_0 in the analytical models. This may be due to site-specific shallow resonance patterns masking part of the effect of attenuation due to damping. An empirical model is developed for the combined V_{S30} and κ_0 scaling for hard-rock sites relative to a reference site condition of 760 m/s (i.e., correction factors that should be used for going from soft rock to hard rock, taking into account the net effect of V_S and κ_0). This empirical model shows high-frequency amplification that is more similar to the analytical prediction corresponding to a hard-rock κ_0 of 0.020 s rather than the typical value of 0.006 s, which is commonly used for hard-rock sites in the central-eastern United States. Compared to the current analytical approach, this leads to a reduction of high-frequency (> 20 Hz) scaling of about a factor of 2.

Online Material: List of records by station and event used for the Swiss (PRP) data; Table of total residuals (in natural log units) at different frequencies computed for the Next Generation Attenuation-East Project (NGA-East) dataset with respect to the Hollenback model; Table of total residuals computed for the BCHydro dataset with respect to the Chiou and Youngs (2014) model; V_S scaling of the Hollenback model for NGA-East.

INTRODUCTION

Estimating ground motion at high frequencies is important for two classes of engineered structures: (1) stiff structures with natural frequencies above 10 Hz, such as small concrete dams where the peak stresses may be controlled by high frequencies (Muto and Duron, 2015), and (2) structures for which safety-related equipment is sensitive to ground shaking at frequencies

above 20 Hz, such as nuclear power plants (e.g., Bandyopadhyay and Hofmayer, 1986).

Characterizing high-frequency ground motion on hard rock empirically is challenging because there are very few ground-motion recordings on such sites (though datasets containing hard-rock data are increasing, for example, the Next Generation Attenuation-East Project [NGA-East] dataset described later); therefore, in practice, analytical models are usually implemented. One approach is to adjust ground-motion prediction equations (GMPEs) from soft-rock conditions, for which there are adequate empirical data, to hard-rock conditions. This adjustment considers the differences in two parameters: (1) the shear-wave velocity of the profile (V_S) and (2) the site-specific high-frequency decay parameter (κ).

κ was first introduced by Anderson and Hough (1984) as the slope measured on the high-frequency part of the acceleration Fourier amplitude spectrum (FAS) of the S waves for a seismic record, when plotted in log-linear space. For an FAS recorded at a given epicentral distance, κ (written here as κ_r) is the combination of site and path attenuation (Hough *et al.*, 1988), similar to t^* . κ_0 is its site-specific component at zero epicentral distance and reflects the attenuation within the first few kilometers beneath a given site (Silva and Darragh, 1995; Campbell, 2009).

If we only account for the differences in the V_S profile (i.e., the impedance contrast) and ignore κ_0 , the computed ground motion will be smaller for hard-rock sites than for soft-rock sites at all frequencies. An example is given in Figure 1a (Biro and Renault, 2012), which shows the pseudospectral acceleration (PSA) amplification based on the point-source stochastic model (PSSM) of Boore (2003), using the quarter-wavelength approach to account for V_S profile differences. If we consider only the effect of κ_0 , then the high-frequency ground motions on hard-rock sites with small κ_0 will be greater than on soft-rock sites, as shown in Figure 1b. Finally, if we consider the combined effect of impedance and damping (V_S and κ_0), then hard-rock sites will have smaller ground motions at low frequencies and larger ground motions at high frequencies, as shown in Figure 1c. Similar scaling effects have been observed in the studies of Van Houtte *et al.* (2011) and Laurendeau *et al.* (2013). Laurendeau *et al.* (2013) also

observed a similar trend in empirically based amplification factors, though the scaling at high frequencies was weaker than shown in Figure 1. Based on this observation, they developed a GMPE that included κ_0 as a predictor variable in addition to V_{S30} .

The database of [Laurendeau *et al.* \(2013\)](#) is composed of soft-rock recordings (National Earthquake Hazards Reduction Program [NEHRP] class B, [Building Seismic Safety Council \[BSSC\], 2003](#)), but no hard-rock recordings (NEHRP class A). Indeed, in most current strong-motion datasets worldwide, the vast majority of data come from stations installed on soil or soft rock (e.g., NGA-West2, see the [Current Models used to Extrapolate to Hard Rock](#) section). Therefore, empirical

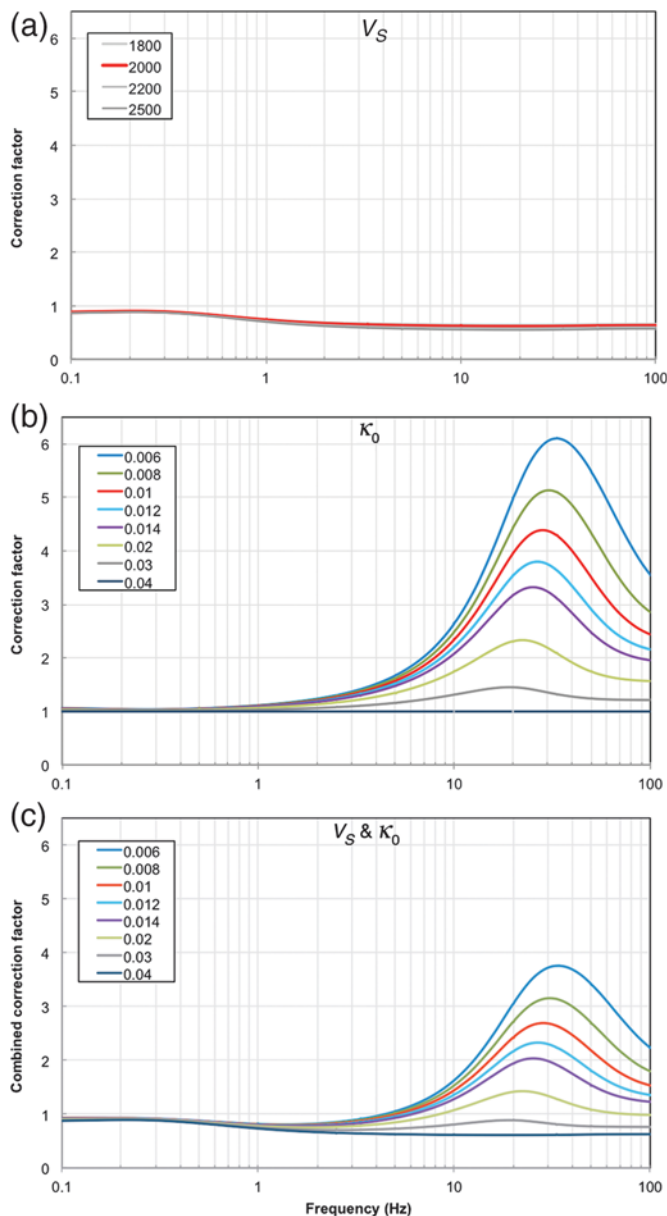
GMPEs derived from such datasets are well constrained for soil and soft-rock sites, but they need to be extrapolated to predict ground motion on hard-rock sites. Because of the lack of data, this extrapolation is usually performed using analytical models rather than extrapolating empirical models. More recordings from hard-rock sites are needed to verify this analytical scaling, or to develop empirically based GMPEs for hard-rock sites that also contain κ_0 as a site predictor.

In this article, we use recently developed datasets that are richer in recordings on hard-rock sites, and we derive empirical scaling factors from soft-rock sites for hard-rock sites. For one of these datasets (NGA-East), κ_0 was computed for all hard-rock stations, so we examine GMPE residuals versus κ_0 . We then estimate the scaling between hard-rock sites ($V_{S30} > 1500$ m/s) and soft-rock sites ($V_{S30} = 760$ m/s), which represents the net effect of site amplification and attenuation (V_{S30} and κ_0). These empirically based hard-rock site factors provide an alternative to the hard-rock site factors based on analytical models.

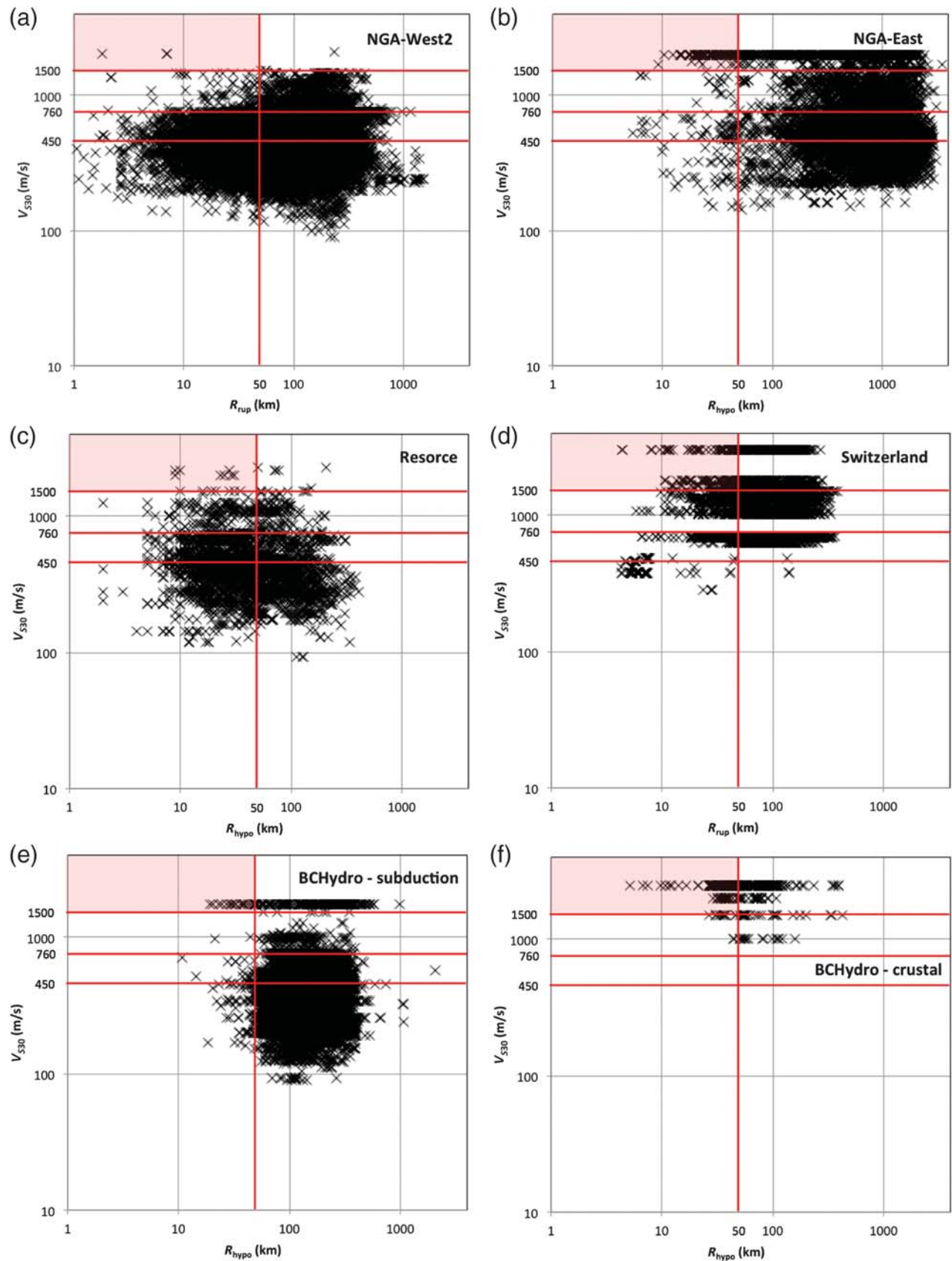
CURRENT MODELS USED TO EXTRAPOLATE TO HARD ROCK

One of the largest and best-documented datasets currently used for shallow crustal seismicity in active regions is the NGA-West2 ([Ancheta *et al.*, 2013](#)). The sampling of V_{S30} in the NGA-West2 dataset is shown in Figure 2 and is summarized in Tables 1 and 2 (italics). As shown in Table 2, of the 21,512 total recordings, only 399 (<2%) are from sites $V_{S30} > 1000$ m/s, and only 7 (<1‰) are from sites with $V_{S30} > 1500$ m/s (i.e., NEHRP class A). If we consider rupture distances within 50 km, to limit the effect of the path attenuation (Q), there are 5966 recordings in the NGA-West2 dataset but just three on sites with $V_{S30} > 1500$ m/s. This shows that there are not enough recordings on hard-rock site conditions to be able to constrain empirically based hard-rock factors using the NGA-West2 data.

In practice, GMPEs are adjusted from soft-rock site conditions to hard-rock site conditions using analytically based site factors (e.g., [Biro and Renault, 2012](#)). This can be done using the hybrid empirical method of [Campbell \(2003, 2004\)](#), where the PSSM is used to estimate the expected differences in the response spectra due to known differences in the seismological parameters and site properties between the host region (region for which the GMPE is derived) and the target region (region for which the ground motion is required). Alternatively, the hard-rock factors can be estimated using the inverse random vibration theory (IRVT) approach of [Al Atik *et al.* \(2014\)](#). In this method, the response spectrum for a soft-rock site condition is converted to the FAS using IRVT; analytically based site corrections that account for the V_S profile and κ_0 differences are applied to the FAS; and then the FAS is converted back to the response spectrum to give the response spectral site factors. In the broadband approach ([Silva *et al.*, 1997](#); details discussed in [Ktenidou *et al.*, 2017](#)), the FAS at all frequencies is fit to a point-source model using a least-squares fit to the log FAS



▲ **Figure 1.** Soft-rock to hard-rock spectral amplification ratios accounting for differences in (a) V_S only, (b) κ_0 only, and (c) combined V_S and κ_0 . Adapted from [Biro and Renault \(2012\)](#).



▲ **Figure 2.** Distribution of hypocentral distance and V_{S30} for the (a) Next Generation Attenuation-West2 Project (NGA-West2), (b) NGA-East, (c) Reference database for Seismic grOund-motion pRediCtion in Europe (RESORCE), (d) Swiss Probabilistic Seismic Hazard Analysis for Swiss Nuclear Power Plant Sites (PEGASOS) Refinement Project (PRP), (e) BCHydro subduction, (f) BCHydro crustal datasets.

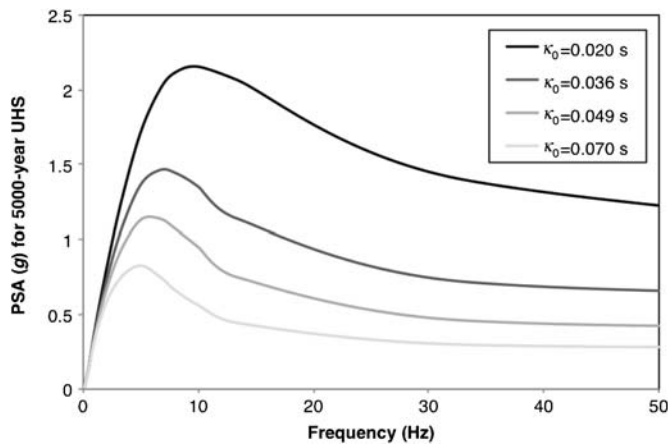
Dataset	Distance R_{hypo}	All Sites	$V_{S30} > 450$ m/s	$V_{S30} > 760$ m/s	$V_{S30} > 1000$ m/s	$V_{S30} > 1500$ m/s
<i>NGA-West2</i>	<i>All</i>	<i>21,512</i>	<i>9329</i>	<i>1204</i>	<i>399</i>	<i>7</i>
	<i><50 km</i>	<i>5966</i>	<i>2166</i>	<i>115</i>	<i>45</i>	<i>3</i>
BCHydro subduction	All	9930	3455	560	254	224
	<100 km	2446	821	172	70	60
BCHydro crustal	<50 km	119	62	28	24	23
	All	322	322	322	322	304
Switzerland PRP	<100 km	270	270	270	270	257
	<50 km	144	144	144	144	142
RESORCE	All	4793	4716	3232	3232	1369
	<100 km	2505	2430	1620	1620	627
NGA-East	<50 km	910	835	569	569	169
	All	2741	1172	274	204	30
RESORCE	<50 km	1623	786	164	125	18
	All	9382	6157	2347	1783	1038
NGA-East	<100 km	408	298	193	178	152
	<50 km	211	167	105	102	87

PRP, Probabilistic Seismic Hazard Analysis for Swiss Nuclear Power Plant Sites (PEGASOS) Refinement Project; RESORCE, REference database for Seismic grOund-motion pRediCtion in Europe.

Dataset	Distance R_{hypo}	$V_{S30} > 450$ m/s (%)	$V_{S30} > 760$ m/s (%)	$V_{S30} > 1000$ m/s (%)	$V_{S30} > 1500$ m/s (%)
<i>NGA-West2</i>	<i>All</i>	<i>43</i>	<i>5.5</i>	<i>1.9</i>	<i><0.1</i>
	<i><50 km</i>	<i>36</i>	<i>2</i>	<i>0.8</i>	<i><0.1</i>
BCHydro subduction	All	35	6	2.6	2.2
	<100 km	34	7	2.9	2.5
BCHydro crustal	<50 km	52	24	20	19
	All	100	100	100	94
Switzerland PRP	<100 km	100	100	100	95
	<50 km	100	100	100	99
RESORCE	All	98	67	67	29
	<100 km	97	65	65	25
NGA-East	<50 km	92	23	20	18.5
	All	43	10	7.4	1.1
RESORCE	<50 km	48	10	7.7	1.1
	All	66	25	19	11
NGA-East	<100 km	73	47	44	37
	<50 km	79	50	48	41

values. Usually, the crustal amplification term is fixed to represent amplification for generic site classes, and the κ_0 for each site (or site class) is one of the point-source model parameters that is estimated as part of the regression.

The value of κ_0 for hard-rock sites can have a large effect on the high-frequency part of the spectrum. As an example, [Muto and Duron \(2015\)](#) show the differences in the 5000-year uniform hazard spectrum (UHS) on a hard-rock site in eastern



▲ **Figure 3.** Effect of κ_0 for hazard on dams according to 5000-year uniform hazard spectrum (UHS). Adapted from Muto and Duron (2015).

California for different κ_0 values (Fig. 3), based on the IRVT method. In this example, the UHS value at 10-Hz spectral acceleration changes by a factor of 2.4 if the estimated site-specific κ_0 for hard-rock changes from 0.02 to 0.05 s.

NEW DATASETS AVAILABLE

In our search for hard-rock data, we review several other current datasets that have recently become available. These comprise the following:

- The European database, REference database for Seismic grOund-motion pRediCtion in Europe (RESORCE; Akkar *et al.*, 2014): This was used to develop several new GMPEs for Europe. Magnitudes range from M 2.6 to 7.8, and R_{hypo} distances from 2 to 402 km. Out of 5637 recordings, about only half come from stations with an estimate of V_{S30} . Of these, 10% are classified as rock (NEHRP class A and B) but only 1% as class A.
- The Probabilistic Seismic Hazard Analysis for Swiss Nuclear Power Plant Sites (PEGASOS) Refinement Project (PRP) database for Switzerland: During the PRP, a database was developed to evaluate the regional effects of ground motions in Switzerland, including the hard-rock site factors. It comprises 4793 recordings (see © Table S1, available in the electronic supplement to this article, for the list of records by station and event), with magnitudes ranging from M 2 to 5.5, distances R_{hypo} from 3 to 370 km, and V_{S30} from 280 to 3010 m/s. Of these, 25% within 100 km are from class A rock sites.
- The BCHydro databases from British Columbia: These comprise one database for crustal and one for subduction seismicity (K. O. Addo, personal comm., 2016). The crustal database comprises 322 recordings, between M 2 and 4.6, R_{hypo} ranging from 5 to 429 km, and recorded exclusively on rock (V_{S30} ranging between 1000 and 2500 m/s). The subduction database comprises 9930 recordings, from an M 4.4 to 8.3 magnitude range, distances

R_{hypo} from 19 to 2060 km, and V_{S30} ranging from 90 to 1750 m/s. Less than 7% of recordings come from sites classified as A or B within 100 km.

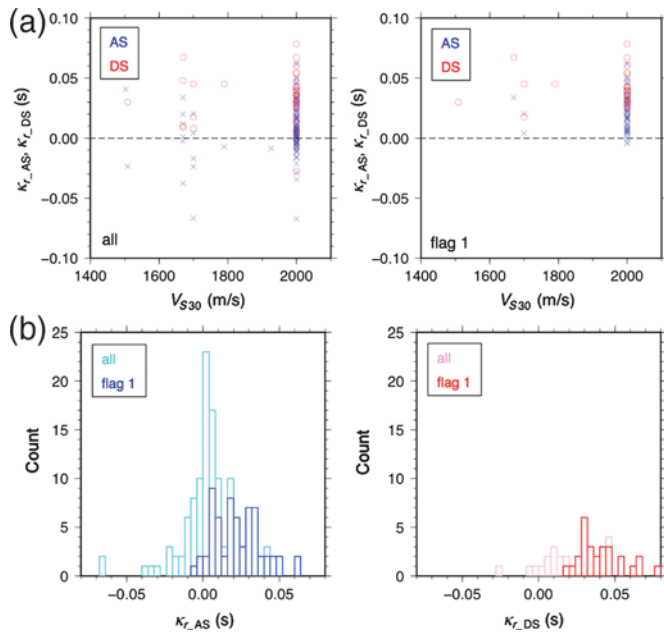
- The NGA-East database: Described in Goulet *et al.* (2014), this dataset contains recordings from the stable continental region of central and eastern North America (CENA). It contains 9382 recordings, magnitudes M 2.1–6.7, and R_{rup} from 4 to 3500 km, from sites with V_{S30} from 200 to 2000 m/s. There are 408 recordings within 100 km. Almost half of the recordings at distances less than 100 km are from site classes A and B, and a third are from site class A.

The distribution of V_{S30} with hypocentral distance for each of these datasets is shown in Figure 2, and the number and percentage of recordings on rock are listed in Tables 1 and 2 (nonitalics). RESORCE cannot offer a significant amount of data for hard rock. However, the NGA-East, BCHydro, and Swiss PRP datasets have enough recordings. Of these, in this article we use the NGA-East and BCHydro datasets, which together offer 229 recordings on hard rock within 50 km, to develop empirically based factors for the combined effect of amplification and attenuation between soft-rock and hard-rock sites.

We note that there is a common problem in most datasets when it comes to characterizing hard-rock sites. Because of the difficulty in measuring V_S profiles at such sites, these are often classified using the general geology of the region. For example, in the NGA-East dataset, of the CENA stations classified as A, almost none have measured V_{S30} values, due to the lack of site characterization in that region. Most of them have been assigned a common value of 2000 m/s (Beresnev and Atkinson, 1997). Similarly, in the BCHydro dataset, all rock sites are classified based on surface geology and using correlations to known V_S profiles from similar geological units.

K_0 FOR NGA-EAST

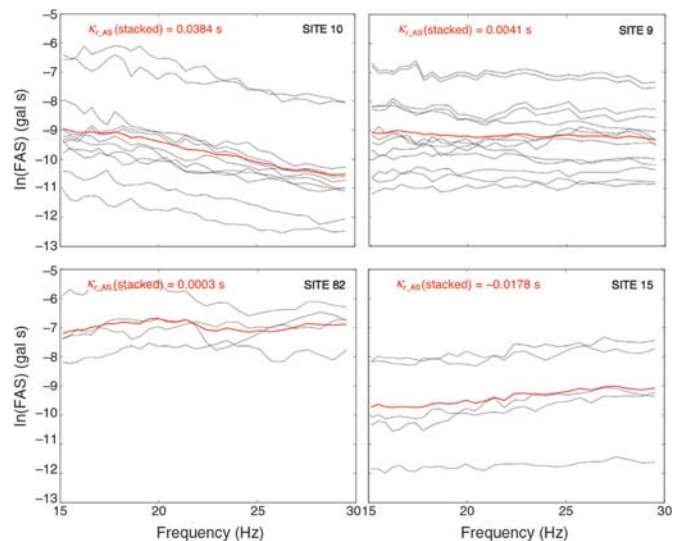
Of the two new datasets that will be used in the following section to study soft-rock to hard-rock scaling, NGA-East is the only one for which we have estimated κ_r values for all of the sites with $V_{S30} > 1000$ m/s at distances closer than 100 km (which can be considered as individual zero-distance κ_0 estimates, because the effect of distance is considered negligible). In Ktenidou, Abrahamson, *et al.* (2016), κ_0 values were estimated with the acceleration spectrum (AS) and the displacement spectrum (DS) method according to the taxonomy of Ktenidou *et al.* (2014), these methods are based, respectively, on the slope of the acceleration FAS, after the original definition of Anderson and Hough (1984), and the slope of the displacement FAS, after the definition of Biasi and Smith (2001). The different approaches are used depending on the corner frequency of earthquake: the AS method is used if the corner frequency is below the 5-to-20 Hz range, and the DS method is used if the corner frequency is above the 5-to-20 Hz range. If the uncertainty in the corner frequency makes the classification ambiguous, then both methods are used. Figure 4a shows



▲ **Figure 4.** (a) $\kappa_{r,AS}$ and $\kappa_{r,DS}$ estimates with V_{S30} for NGA-East hard-rock stations, considering all records (left), and only records with downtrending, flag-1 Fourier amplitude spectrum (FAS; right). Note that the concentration of data points at 2000 m/s is due to the empirical assignment of this value to most hard-rock central and eastern North America sites. (b) Histograms showing the range of κ estimates for the acceleration FAS (AS; teal, all records; blue, flag-1 records) and displacement FAS (DS) approaches (pink, all records; red, flag-1 records). All records are within 100 km.

estimated κ_r values with V_{S30} for both approaches, and Figure 4b shows the distribution of measured values per approach. There can be systematic differences in the κ_r values according to the measurement approach used, namely the DS approach (red points, $\kappa_{r,DS}$) tends to lead to higher κ_r compared to the traditional AS approach (blue points, $\kappa_{r,AS}$) for events in which the uncertainty in the corner frequency allows both approaches to be used. However, within each approach, the scatter is still very large, and because most of the class A sites have been assigned a single V_{S30} value of 2000 m/s, it is not possible to observe a correlation of κ_r with V_{S30} for hard-rock sites. It is not clear how much of the scatter in the κ_r measurements is due to differences in V_{S30} values for the hard-rock sites.

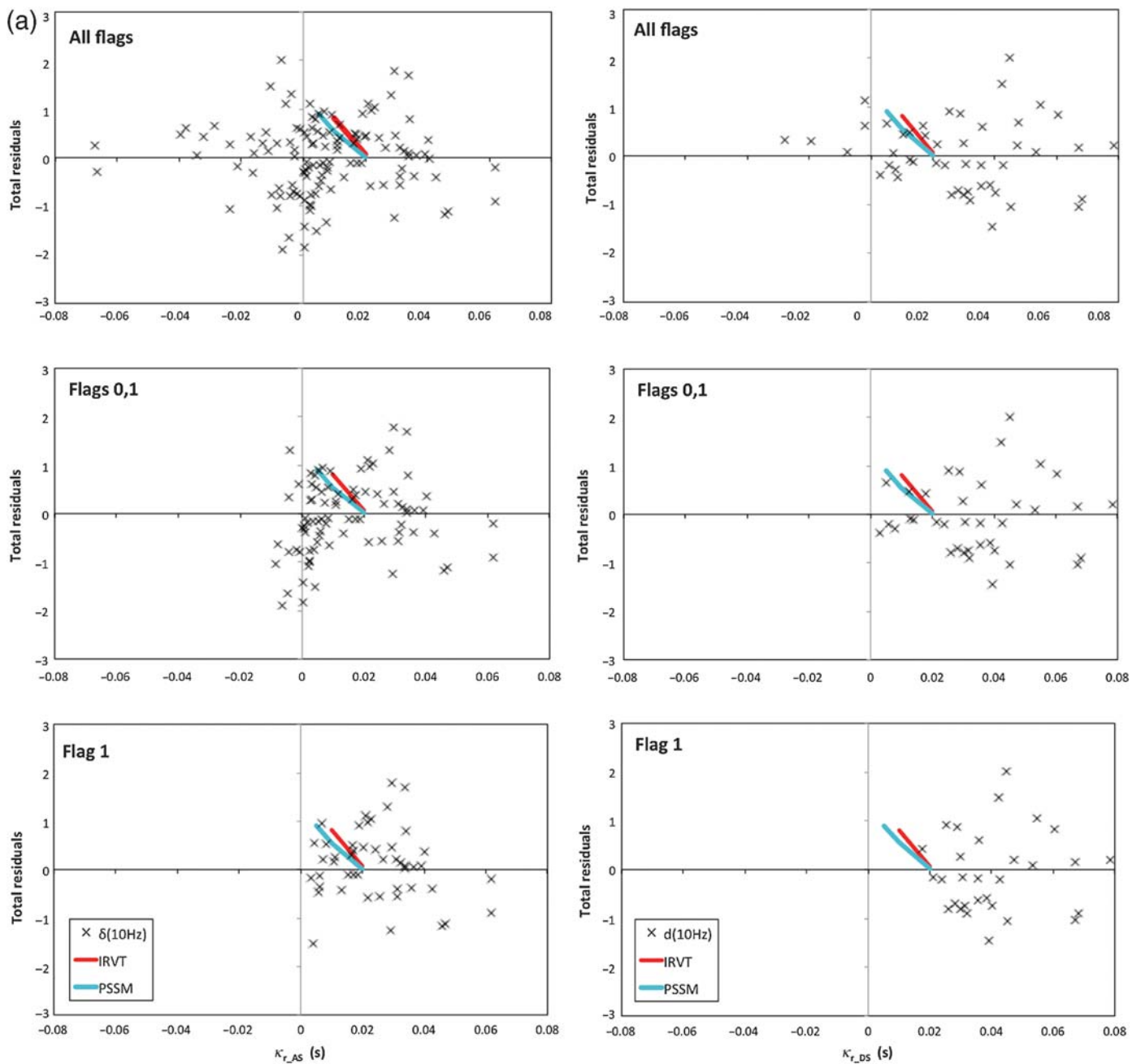
Parolai and Bindi (2005) first cautioned against measuring κ on a FAS whose shape is strongly distorted by shallow resonance, because the value can be biased near strong amplification peaks caused by shallow impedance contrast. Ktenidou, Abrahamson, *et al.* (2016) found that amplification effects may also be present in rock sites, and that there may be correlations between site amplification and site attenuation in what is measured as κ_r for hard rock. Figure 5 shows the FAS of acceleration for some hard-rock sites in CENA, on which κ_r was measured using the AS approach. At sites 10 and 9 (both have assigned $V_{S30} = 2000$ m/s), the FAS show a downward trend above 15 Hz, but this is stronger in the first



▲ **Figure 5.** Mean FAS derived from stacking all recordings per station for the AS approach, and estimation of mean κ_0 per site (red). Individual FAS are shown in black. The station number is written on the top right.

case and weaker in the second. If we average all κ_r estimates per station, the resulting mean κ_0 values per station are 0.038 and 0.004 s, respectively, depending on whether we include only downtrending FAS or all FAS. These κ_0 values are close to the typical values assumed up to now for the western United States (0.040 s according to Boore, 2003; Atkinson and Silva, 1997) and the eastern United States (0.006 s according to Campbell *et al.*, 2014). On the other hand, at sites 82 and 15, the FAS do not exhibit clear decay up to 30 Hz, and the mean $\kappa_{0,AS}$ values can be near zero (0.0003 s) or even negative (−0.017 s). This observation is consistent over the FAS from multiple earthquakes recorded at these stations. Therefore, the low or negative κ_0 values may be due to broadband amplification effects at high frequencies at those stations; these could give the FAS an upward trend and partially or completely mask the downward trend expected of the FAS due to the damping. This implies that the measured κ_0 value, which is subsequently used as a proxy of attenuation only, reflects the combined effect of damping and other factors that are not captured in the average amplifications assumed for the hard-rock sites.

In Ktenidou, Abrahamson, *et al.* (2016), FAS were visually inspected and assigned flags to indicate their high-frequency trend: −1 for upgoing, 0 for near-horizontal, and 1 for downgoing FAS. The mean κ_0 values estimated over the entire NGA-East hard-rock dataset depended strongly on whether the FAS of all flags were considered. If all flags are considered (*i.e.*, also recordings for which damping is masked by amplification or other phenomena), then the mean $\kappa_{0,AS}$ value over the ensemble of sites is 0.006–0.008 s, depending on stacking, and is similar to the typical κ_0 value assumed up to now for CENA hard rock (0.006 s); but if only the downtrending FAS are considered, then the mean $\kappa_{0,AS}$ value over all sites is much higher, ranging from 0.019 to 0.025 s. This result is consistent



▲ **Figure 6.** Total residuals for the Hollenback model versus measured (left) $\kappa_{r_{AS}}$ values and (right) $\kappa_{r_{DS}}$ values for all recordings (top), recordings without significant upgoing trend in their FAS (middle), and recordings with clear downgoing trend in their FAS (bottom). The blue and red lines show the theoretical scaling predicted from the point-source stochastic model (PSSM) and inverse random vibration theory (IRVT), respectively. (a) 10 Hz, (b) 20 Hz, and (c) 30 Hz. *(Continued)*

regardless of whether we measure κ for each record individually and then average them, or whether we measure κ using stacked recordings at each station and then average them.

Using the κ_0 values from Ktenidou, Abrahamson, *et al.* (2016), we evaluate the dependency of the response spectrum residuals with κ_0 . The total residuals (see the  electronic supplement) are computed with respect to the empirical GMPE that was created by J. Hollenback for studying standard deviations in CENA (Al Atik, 2015, chap. 3; we stress here that this

GMPE is not meant to be extrapolated for predictions outside the range of its data). As a site term, the effects of κ should be correlated with the within-event residuals; however, there may be a correlation of κ with the event terms if the κ values are spatially correlated (e.g., if all recordings from an earthquake are from low κ_0 sites, then the average effect of κ_0 would be manifested in the event term).

Figure 6a–c shows the hard-rock ($V_{S30} > 1500$ m/s) total residuals at high frequencies (10, 20, and 30 Hz) against the

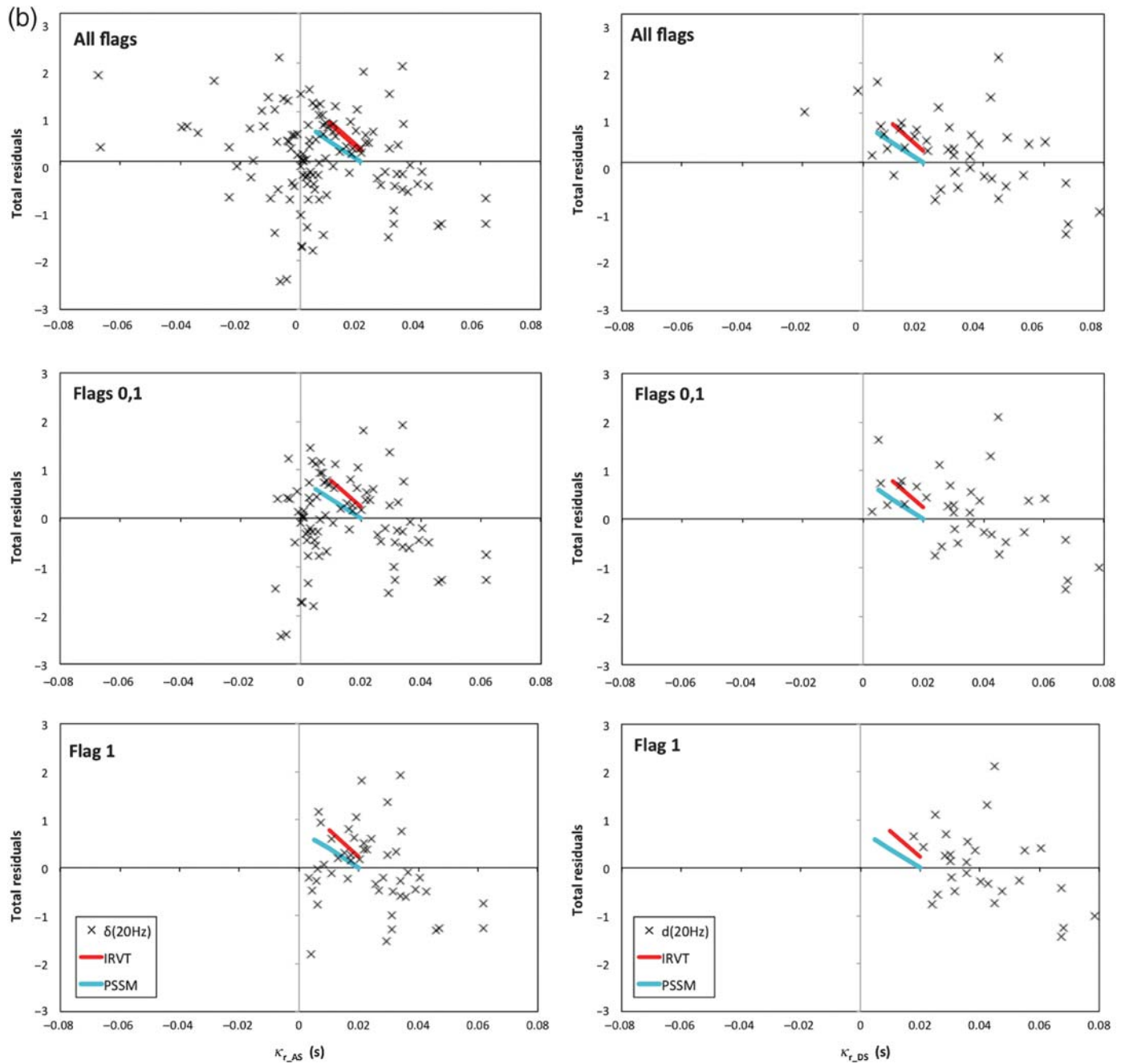


Figure 6. Continued.

estimated κ_0 values for sites at distances of less than 100 km. The two lines indicate the theoretical scaling of total residuals with κ_0 , as predicted from the PSSM (blue line, from 0.020 to 0.005 s) and from the IRVT approach (red line, from 0.020 to 0.010 s) mentioned above. If the site factor for hard-rock sites scales strongly with κ_0 as indicated by the modeling, then we expect to see a strong negative correlation of the residuals versus κ_0 , because small κ_0 values will lead to higher ground motions and, therefore, larger residuals. When it comes to the $\kappa_{r,AS}$ values (left panels of Fig. 6a–c), the residuals between κ_0 of 0.005 and 0.020 s do not show the strong trend that

is predicted by the analytical models. That is, the high-frequency response spectral values of the NGA-East hard-rock data do not show the expected dependence on κ_0 , when κ_0 is computed with the AS approach. However, the residuals with respect to $\kappa_{r,DS}$ measurements (right panels of Fig. 6a–c) do show a trend with κ_0 that is more consistent with the theoretical scaling.

To interpret this observation, we note that $\kappa_{r,AS}$ and $\kappa_{r,DS}$ are measured over different frequency bands. $\kappa_{r,AS}$ was measured on the AS mostly in the 15–35 Hz range, whereas $\kappa_{r,DS}$ was measured on the DS mostly in the 5–15 Hz range.

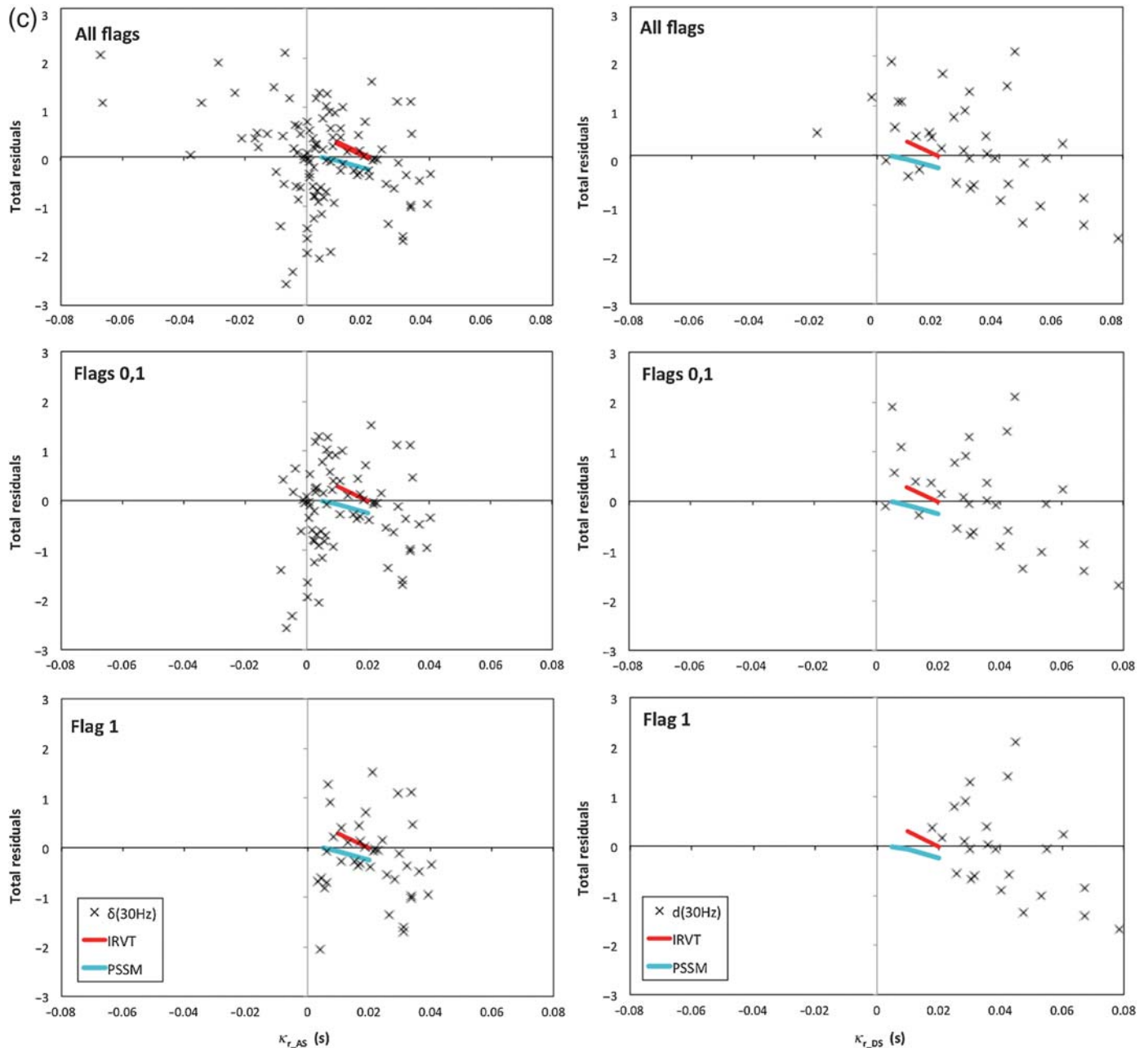
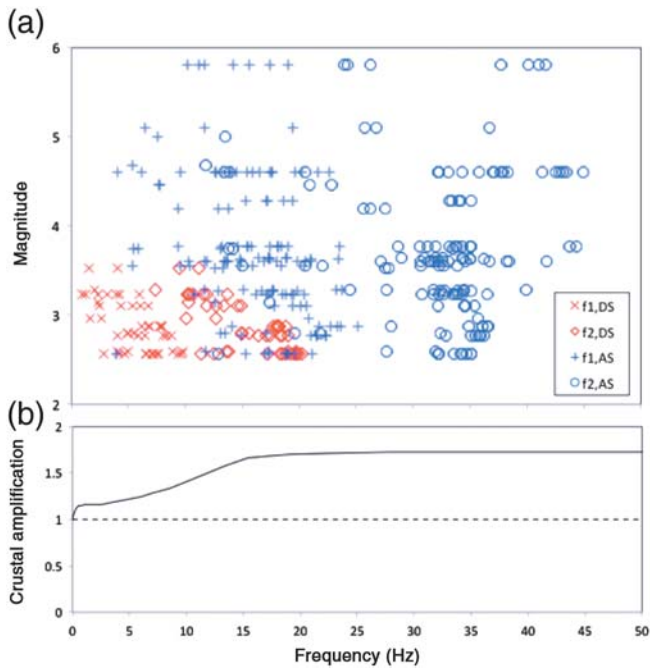


Figure 6. Continued.

Figure 7 shows the lower (f_1) and upper (f_2) frequency used to estimate κ for each recording, with each approach. This figure also shows the crustal amplification transfer function, which was computed for the generic hard-rock profile in CENA, and which was used to correct all FAS before estimating κ . Figure 8 shows a comparison of measured κ_{r_AS} (a) and κ_{r_DS} (b) for site-corrected and uncorrected FAS; in the former case, there is no perceivable difference, whereas in the latter there is a systematic shift in the values before and after correction. The assumed crustal amplification (shown in Fig. 7b) has a slope below 15 Hz, so the correction of the FAS due to the V_S profile mostly affects the results of the DS approach. It is possible that

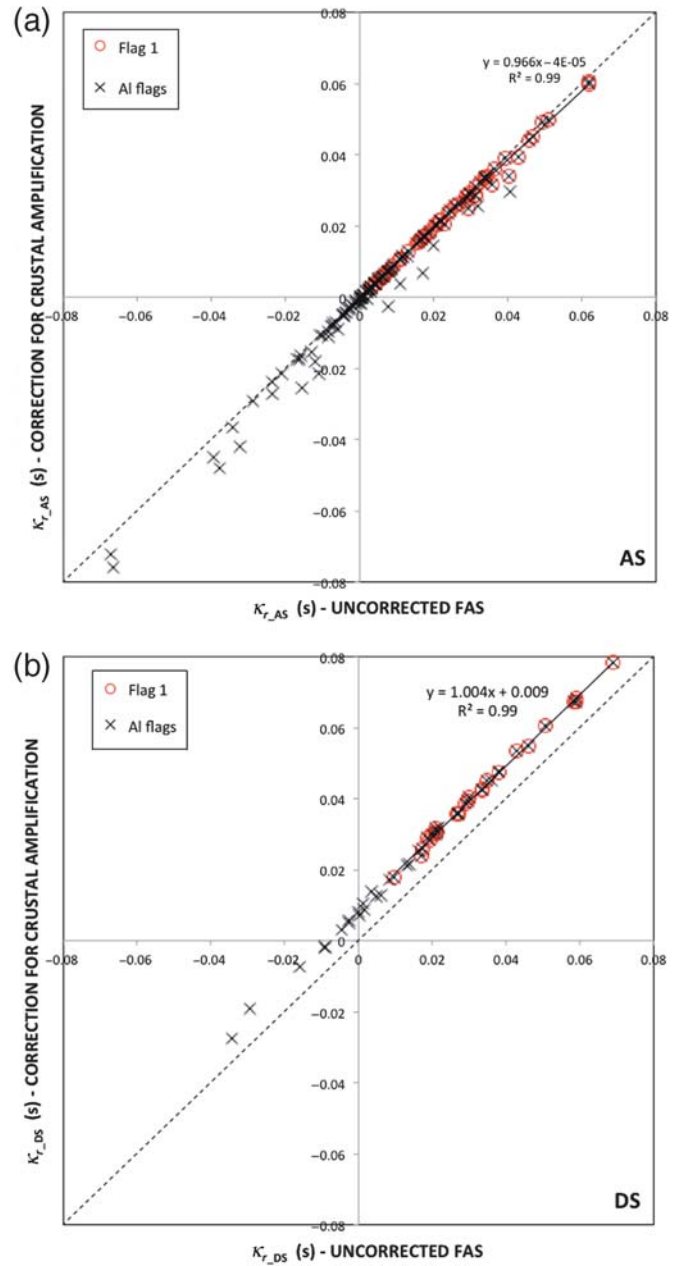
there is crustal amplification above 15 Hz, which is not captured by the generic V_S profile used for hard-rock sites due to lack of small-scale information that would affect high frequencies. In this case, it would mean that the κ_{r_DS} measurements better reflect the damping in the shallow crust, whereas the κ_{r_AS} measurements may rather reflect a net effect of damping and amplification, which has not been decoupled. This would imply that, with improved site characterization at hard-rock sites, the crustal amplification above 15 Hz could be used to correct the FAS above 15 Hz. With an improved site characterization, the residuals might scale more strongly with κ_{r_AS} values, as they do with κ_{r_DS} values.



▲ **Figure 7.** (a) Lower and upper-frequency limits (f_1 and f_2) used to measure $\kappa_{r_{AS}}$ (blue symbols) and $\kappa_{r_{DS}}$ (red symbols) for NGA-East hard-rock sites shown in Figure 8, plotted against magnitude. (b) The crustal amplification function, which mainly affects the band for $\kappa_{r_{DS}}$.

EMPIRICAL SCALING MODEL FROM SOFT ROCK TO HARD ROCK

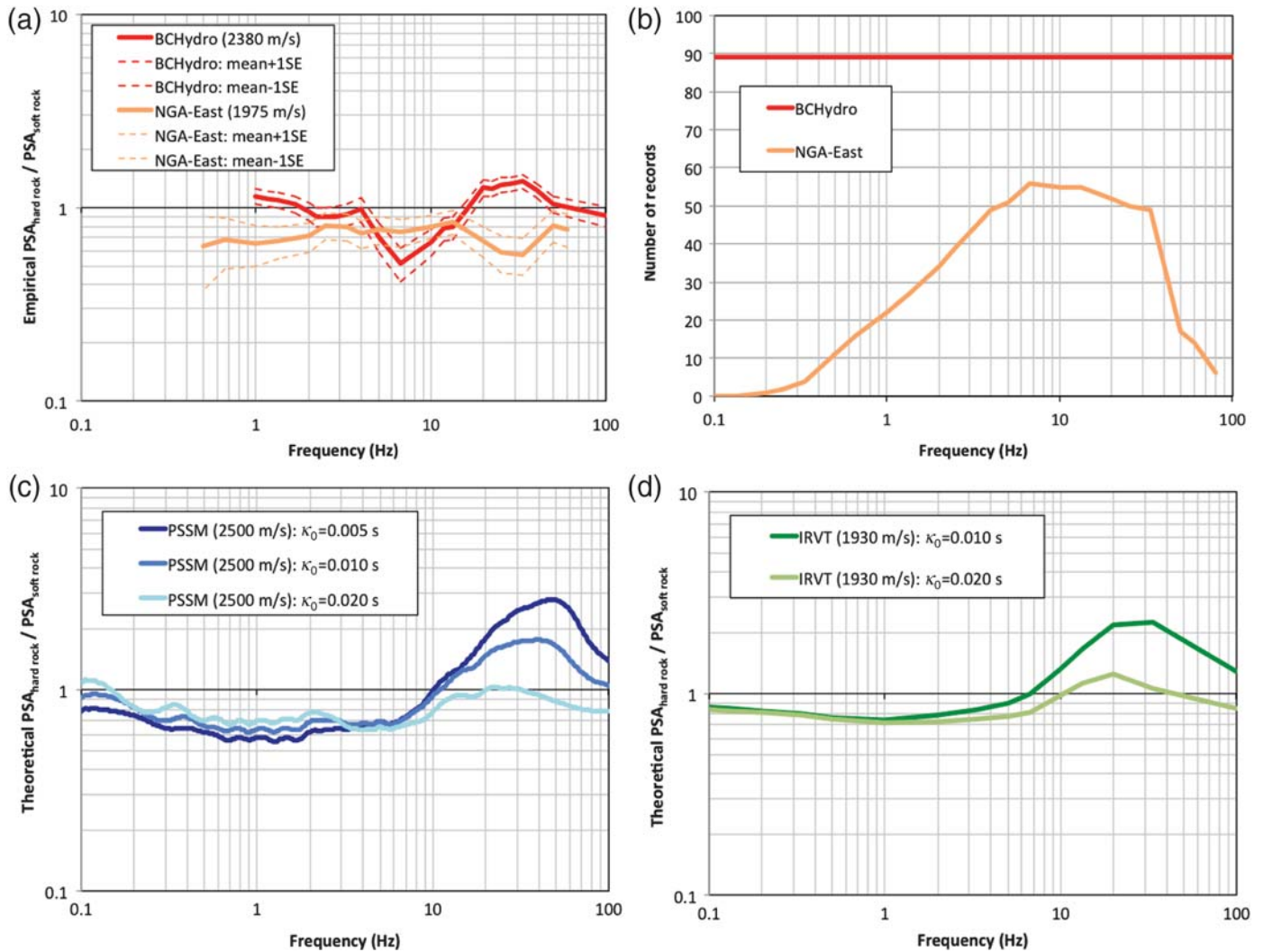
Given that we do not see strong κ_0 scaling in the NGA-East residuals and that there are known trade-offs between κ_0 and amplification (so it is difficult to decouple κ_0 effects from V_{S30} scaling), we use the NGA-East and BCHydro data to develop an empirical model for the combined effect of V_S profile and κ_0 with respect to a soft-rock site ($V_{S30} = 760$ m/s). We consider the subsets of recordings within 50 km (rows 8 and 16 of Table 1) to minimize the effect of path attenuation (Q), and for NEHRP class A sites (last column in the table). We only consider earthquakes with magnitudes above M 3, because the GMPEs used to compute the residuals are not constrained well below this threshold. For each of the two datasets, we compute total residuals with respect to an appropriate GMPE, but we substitute the sites' actual V_{S30} values with a reference soft-rock value of 760 m/s. The resulting residuals reflect the net difference in the site response between hard-rock and soft-rock sites. We use total rather than within-event residuals to avoid bias from potential trade-offs between site and event terms. For the NGA-East, we use the Hollenback model mentioned above, whereas for the BCHydro dataset we use the GMPE of Chiou and Youngs (2014). For each dataset, we compute the mean residual per frequency over all available recordings, giving equal weight to each recording (individual residual values for NGA-East and BCHydro can be found in Tables S2 and S3, respectively). The V_S scaling for the BCHydro GMPE can be



▲ **Figure 8.** Comparison of measured (a) $\kappa_{r_{AS}}$ and (b) $\kappa_{r_{DS}}$ for site-corrected and uncorrected FAS.

found in Chiou and Youngs (2014), whereas the V_S scaling of the NGA-East GMPE is given in Table S4.

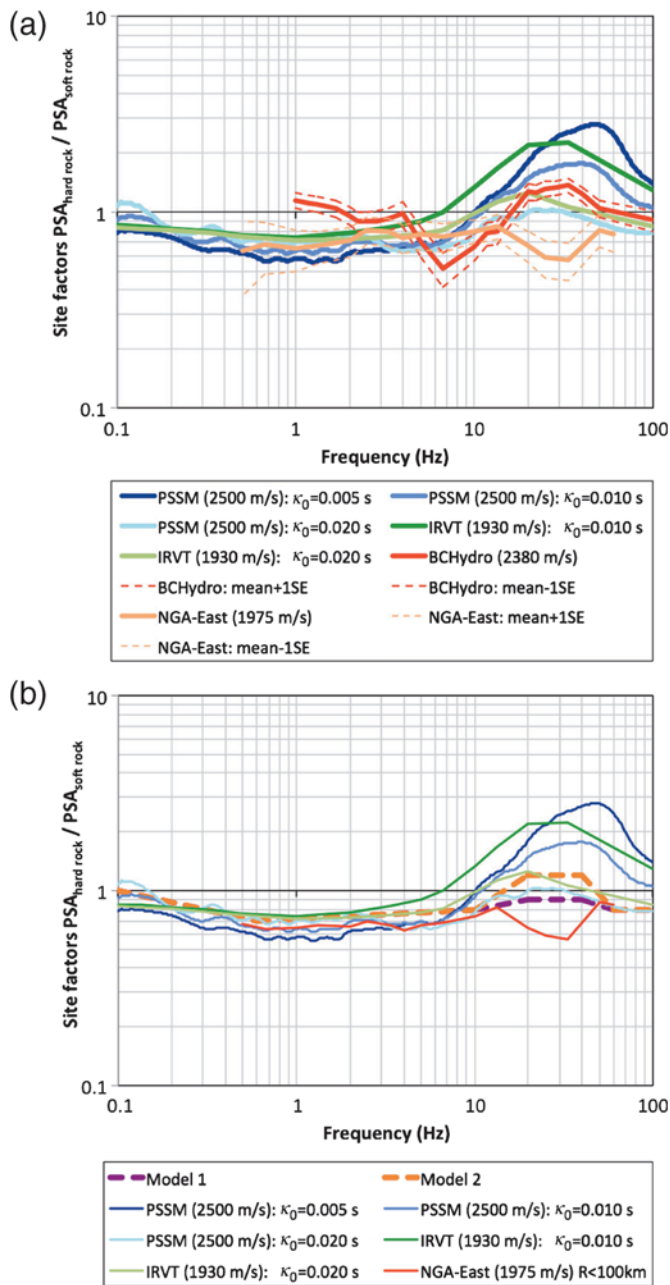
The mean residuals are used to compute the V_S - κ_0 site factors (i.e., the site factors that should be used for going from soft rock to hard rock, taking into account the net effect of V_S and κ_0 , labeled here $PSA_{\text{hard rock}}/PSA_{\text{soft rock}}$). In Figure 9a, at low frequencies (e.g., 0.5–3 Hz), the factors are in the 0.6–0.9 range, consistent with the scaling for the change in the impedance contrast. At high frequencies (e.g., 20–40 Hz), for BCHydro there is some amplification (maximum of 1.3) in the 20–50 Hz range consistent with a reduced κ_0 for hard-rock sites compared



▲ **Figure 9.** (a) Site factors from soft rock to hard rock ($PSA_{\text{hard rock}}/PSA_{\text{soft rock}}$) using the BCHydro and NGA-East datasets out to 50 km, for magnitudes M 3 and above, and for sites in National Earthquake Hazards Reduction Program class A ($V_{S30} \geq 1500$ m/s). Dashed lines indicate the standard error. (b) Number of recordings available per frequency. (c) Theoretical soft-rock to hard-rock amplification factor on pseudospectral acceleration (PSA) using the PSSM and (d) for the IRVT approaches.

to soft-rock sites. For NGA-East, however, there is no amplification above 20 Hz; the $V_S-\kappa_0$ site factor ranges between 0.6 and 0.8. Figure 9a implies that we do not observe strong scaling at high frequencies between soft-rock and hard-rock sites as predicted by the commonly used analytical methods. These results, obtained for recordings within 50 km, do not vary significantly if we consider recordings out to 100 km, considering the standard errors shown as dashed lines in the figure. We only show mean residuals at frequencies for which there are at least 10 usable recordings (Fig. 9b). For BCHydro, we consider the results reliable above 5 Hz; the amplification greater than unity at 1 Hz is not consistent with the expected low-frequency scaling between hard-rock and soft-rock sites. This is because of magnitude estimation issues for small events, which may inflate residuals at frequencies below the source corner frequency (so for M 3, up to 5–10 Hz).

In Figure 9c,d, we show the analytical site factors based on the PSSM simulations and the IRVT approach. In Figure 10a, we overlay our empirical site factors onto the analytical site factors. The latter predict stronger scaling from hard-rock to soft-rock sites. We find that our empirical results for BCHydro correspond to the analytical results if we assume that hard-rock sites have κ_0 values close to 0.015–0.020 s rather than the typical assumed value of 0.006 s. For NGA-East, the results would indicate even higher κ_0 values, above 0.020 s. We believe that this may be due to the measured κ_0 values not reflecting only damping but a net effect of damping and amplification. This implies that when selecting κ_0 values to adjust soft-rock ground-motion models to hard-rock site conditions, considering only the damping effect may lead to overestimation of the κ_0 effects. The scaling model in Figure 10a includes the net effect of V_S and κ_0 .



▲ **Figure 10.** (a) Overlay of empirical and theoretical site factors ($PSA_{\text{hard rock}}/PSA_{\text{soft rock}}$). Dashed lines indicate the standard error for the empirical estimates. (b) Proposed empirical model for $PSA_{\text{hard rock}}/PSA_{\text{soft rock}}$ site factors.

Based on these comparisons, we develop two models for the hard-rock scale factors at high frequencies (Fig. 10b; Table 3). For both models, the low-frequency range follows the NGA-East amplification, because this is more stable and not affected by magnitude scaling issues. At high frequencies, the first model (orange line) follows the BCHydro amplification and represents our upper range of amplification. The second model (purple line) is the smooth weighted average of the amplifications of the two empirical datasets. Similar amplification

Frequency (Hz)	0.1	0.6	10	20	40	60	100
Model 1	1	0.7	0.8	0.9	0.9	0.8	0.8
Model 2	1	0.7	0.8	1.2	1.2	0.8	0.8

factors can be developed using analytical modeling using hard-rock κ_0 values of 0.015–0.025 s.

CONCLUSIONS AND PERSPECTIVES

The proposed V_S - κ_0 scaling for hard-rock sites related to a reference V_{S30} of 760 m/s given in Table 3 can be used as an alternative to the currently used analytical models. Using analytical models with $\kappa_0 = 0.02$ s will lead to combined V_S - κ_0 scaling generally consistent with the currently available hard-rock data.

A key limitation of the proposed hard-rock site factors is the relatively small dataset available. From our review of available datasets for hard-rock ground motions, it is clear that there is a need for additional data from hard-rock sites, and there is a need to better characterize hard-rock sites. Most datasets for active crustal regions in Europe and the United States (with the exception of BCHydro) contain less than 10% of rock data (NEHRP classes B and above), and less than 3% hard-rock data (class A), whereas datasets for stable continental regions contain more than 10% hard-rock data. Of these recordings, some come from stations that are poorly characterized. For instance, for some datasets (RESORCE and Swiss PRP), half of the V_{S30} values are still missing, whereas for the NGA-East and BCHydro, almost all hard-rock stations have an assigned rather than a measured V_{S30} value.

In this article, we have not examined downhole data. We believe recordings from downhole stations have the potential to significantly increase the number of available data on hard rock (e.g., KiK-net stations at 100 and 200 m, Aoi *et al.*, 2004; Treasure Island Array, Graizer, 2014). Ktenidou *et al.* (2015) used downhole stations on hard rock to suggest that hard-rock κ_0 values may reach an asymptotic value that is region dependent. If this suggestion is confirmed by more data, then future studies could integrate global hard-rock datasets and assess them consistently, with the goal of characterizing hard-rock response in different regions. Denser permanent instrumentation, including downhole instrumentation, can also help better understand the dispersion in measured κ_0 values and to decouple the trade-off between site attenuation and site amplification.

We also note the need for higher sampling rates and higher low-pass anti-alias filters, which will allow analysis of data at higher frequencies. This could help resolve issues of trade-off, not only between site attenuation and amplification at hard sites with high-frequency resonance patterns but also between site attenuation and source corner frequency or stress drop. For instance, for the NGA-East, most data come

from the Transportable Array (see [Data and Resources](#)), for which the highest usable frequency is only 16 Hz (Ktenidou *et al.*, 2017).

DATA AND RESOURCES

The metadata of REference database for Seismic grOund-motion pRediCtion in Europe (RESORCE) dataset can be accessed by registered users at <http://www.resorce-portal.eu/> (last accessed December 2015), and for Next Generation Attenuation-West2 Project (NGA-West2) and NGA-East they are publicly accessible at <http://peer.berkeley.edu/ngawest2/databases/> (last accessed December 2015) and <http://peer.berkeley.edu/ngaeast/technical-updates/2014-fourth/> (last accessed December 2015), respectively. Metadata for the other datasets were provided by BCHydro and swissnuclear. The list of records in © Table S3 can be used to retrieve the event parameters from the Swiss Seismological Service catalog (<http://hitseddb.ethz.ch:8080/ecos09/query>, last accessed June 2016). For the NGA-East, most data come from the Transportable Array accessible at <http://www.usarray.org/researchers/obs/transportable> (last accessed September 2015). ☒

ACKNOWLEDGMENTS

This article is dedicated to the memory of Stephen P. Ktenides (1926–2016).

We thank W. Silva, R. Darragh, J. Hollenback, D. Bindi, M. Muto, T. Kishida, K. Addo, F. Cotton, A. Laurendeau, S. Bora, and C. Di Alessandro for discussions, and Ph. Renault for an internal review. We also thank Associate Editor Martin Chapman. This article was improved thanks to comments by Ivan Wong and an anonymous reviewer. Finally, we thank BCHydro, swissnuclear, and Pacific Earthquake Engineering Research Center (PEER) for providing summaries of their datasets. This study was funded by Pacific Gas & Electric Company (PG&E).

REFERENCES

Akkar, S., M. A. Sandikkaya, M. Senyurt, A. Azari Sisi, B. Ö. Ay, P. Traversa, J. Douglas, F. Cotton, L. Luzi, B. Hernandez, *et al.* (2014). Reference database for seismic ground-motion in Europe (RESORCE), *Bull. Earthq. Eng.* **12**, 311–339.

Al Atik, L. (2015). NGA-East: Ground-motion standard deviation models for central and eastern North America, *PEER Report 2015/07*, Pacific Earthquake Engineering Research Center, available at http://peer.berkeley.edu/publications/peer_reports/reports_2015/webPEER-2015-09-moustafa.pdf (last accessed June 2016).

Al Atik, L., A. Kottke, N. Abrahamson, and J. Hollenback (2014). Kappa correction of ground motion prediction equations using inverse random vibration theory approach, *Bull. Seismol. Soc. Am.* **104**, 336–346.

Ancheta, T. D., R. B. Darragh, J. P. Stewart, E. Seyhan, W. J. Silva, B. S. J. Chiou, K. E. Wooddell, R. W. Graves, A. R. Kottke, D. M. Boore, *et al.* (2013). PEER NGA-West2 database, *PEER Report 2013/03*, Pacific Earthquake Engineering Research Center, available at http://peer.berkeley.edu/publications/peer_reports/reports_2013/webPEER-2013-03-Ancheta.pdf (last accessed June 2016).

Anderson, J. G., and S. E. Hough (1984). A model for the shape of the Fourier amplitude spectrum of acceleration at high frequencies, *Bull. Seismol. Soc. Am.* **74**, 1969–1993.

Aoi, S., T. Kunugi, and H. Fujiwara (2004). Strong-motion seismograph network operated by NIED: K-NET and KiK-net, *J. Japan Assoc. Earthq. Eng.* **4**, 65–74.

Atkinson, G. M., and W. J. Silva (1997). An empirical study of earthquake source spectra for California earthquakes, *Bull. Seismol. Soc. Am.* **87**, 97–113.

Bandyopadhyay, K. K., and C. H. Hofmayer (1986). *Seismic Fragility of Nuclear Power Plant Components (Phase 1)*, The Commission, Washington, D.C.

Beresnev, I. A., and G. M. Atkinson (1997). Shear-wave velocity survey of seismographic sites in eastern Canada: Calibration of empirical regression method of estimating site response, *Seismol. Res. Lett.* **68**, 981–987.

Biasi, G. P., and K. D. Smith (2001). Site Effects for Seismic Monitoring Stations in the Vicinity of Yucca Mountain, Nevada, MOL20011204.0045, a report prepared for the US DOE/University and Community College System of Nevada (UCCSN) Cooperative Agreement.

Biro, Y., and P. Renault (2012). Importance and impact of host-to-target conversions for ground motion prediction equations in PSHA, *Proc. of the 15th World Conf. of Earthquake Engineering*, Lisbon, Portugal.

Boore, D. M. (2003). Simulation of ground motion using the stochastic method, *Pure Appl. Geophys.* **160**, 635–676.

Building Seismic Safety Council (BSSC) (2003). The 2003 NEHRP Recommended Provisions for New Buildings and Other Structures (FEMA 450). Part 1: Provisions, Federal Emergency Management Agency, Washington, D.C., available at <http://bssc.nibs.org> (last accessed June 2016).

Campbell, K. W. (2003). Prediction of strong ground motion using the hybrid empirical method and its use in the development of ground-motion (attenuation) relations in eastern North America, *Bull. Seismol. Soc. Am.* **93**, 1012–1033.

Campbell, K. W. (2004). Erratum: Prediction of strong ground motion using the hybrid empirical method and its use in the development of ground-motion (attenuation) relations in eastern North America, *Bull. Seismol. Soc. Am.* **94**, 2418.

Campbell, K. W. (2009). Estimates of shear-wave Q and κ_0 for unconsolidated and semiconsolidated sediments in eastern North America, *Bull. Seismol. Soc. Am.* **99**, 2365–2392.

Campbell, K. W., Y. M. A. Hashash, B. Kim, A. R. Kottke, E. M. Rathje, W. J. Silva, and J. P. Stewart (2014). Reference-rock site conditions for Central and Eastern North America: Part II—Attenuation (Kappa) definition, *PEER Report 2014/12*, Pacific Earthquake Engineering Research Center, available at peer.berkeley.edu/publications/peer_reports/reports_2014/webPEER-2014-12-Campbell.pdf (last accessed June 2016).

Chiou, B. S. J., and R. R. Youngs (2014). Update of the Chiou and Youngs NGA model for the average horizontal component of peak ground motion and response spectra, *Earthq. Spectra* **30**, 1117–1153.

Goulet, C., T. Kishida, T. D. Ancheta, C. H. Cramer, R. B. Darragh, W. J. Silva, Y. M. A. Hashash, J. Harmon, J. P. Stewart, K. E. Wooddell, *et al.* (2014). PEER NGA-East database, *PEER Report 2014/17*, Pacific Earthquake Engineering Research Center, available at http://peer.berkeley.edu/publications/peer_reports/reports_2014/webPEER-2014-17-NGA-East-Database.pdf (last accessed June 2016).

Graizer, V. (2014). Comment on “Comparison of Time Series and Random-Vibration Theory Site-Response Methods” by Albert R. Kottke and Ellen M. Rathje, *Bull. Seismol. Soc. Am.* **104**, 540–546.

Hough, S. E., J. G. Anderson, J. Brune, F. Vernon III, J. Berger, J. Fletcher, L. Haar, T. Hanks, and L. Baker (1988). Attenuation near Anza, California, *Bull. Seismol. Soc. Am.* **78**, 672–691.

Ktenidou, O.-J., N. Abrahamson, R. Darragh, and W. Silva (2016). A methodology for the estimation of kappa (κ) from large datasets, example application to rock sites in the NGA-East database, and implications

- on design motions, *PEER Report 2016/01*, Pacific Earthquake Engineering Research Center, available at peer.berkeley.edu/publications/peer_reports/reports_2016/webPEER-2016-01-ktenidou.pdf (last accessed June 2016).
- Ktenidou, O.-J., N. Abrahamson, S. Drouet, and F. Cotton (2015). Understanding the physics of kappa (κ): Insights from a downhole array, *Geophys. J. Int.* **203**, 678–691.
- Ktenidou, O.-J., F. Cotton, N. A. Abrahamson, and J. G. Anderson (2014). Taxonomy of κ : A review of definitions and estimation approaches targeted to applications, *Seismol. Res. Lett.* **85**, 135–146.
- Ktenidou, O.-J., W. Silva, R. Darragh, N. Abrahamson, and T. Kishida (2017). Squeezing kappa out of the Transportable Array in a low seismicity region, *Bull. Seismol. Soc. Am.*, doi: [10.1785/0120150301](https://doi.org/10.1785/0120150301).
- Laurendeau, A., F. Cotton, O.-J. Ktenidou, L.-F. Bonilla, and F. Hollender (2013). Rock and stiff-soil site amplification: Dependencies on V_{s30} and kappa (κ_0), *Bull. Seismol. Soc. Am.* **103**, 3131–3148.
- Muto, M., and Z. Duron (2015). High-frequency seismic hazard estimation and impact on seismic evaluation for dams (SSA Annual Meeting), *Seismol. Res. Lett.* **86**, no. 2B, 651.
- Parolai, S., and D. Bindi (2004). Influence of soil-layer properties on k evaluation, *Bull. Seismol. Soc. Am.* **94**, 349–356.
- Silva, W. J., and R. Darragh (1995). *Engineering Characterization of Earthquake Strong Ground Motion Recorded at Rock Sites*, Electric Power Research Institute, Palo Alto, California, TR-102261.
- Silva, W. J., N. A. Abrahamson, G. Toro, and C. Costantino (1997). Description and validation of the stochastic ground motion model, *Report Submitted to Brookhaven National Laboratory, Contract No. 770573*, Associated Universities, Inc., Upton, New York, available at http://www.pacificengineering.org/rpts_page1.shtml (last accessed June 2016).
- Van Houtte, C., S. Drouet, and F. Cotton (2011). Analysis of the origins of κ (kappa) to compute hard rock to rock adjustment factors for GMPEs, *Bull. Seismol. Soc. Am.* **101**, 2926–2941.

Olga-Joan Ktenidou
University of Greenwich
Department of Engineering Science
Central Avenue, Chatham Maritime
Kent ME4 4TB, United Kingdom
o.ktenidou@gre.ac.uk

Norman A. Abrahamson
Pacific Gas & Electric Company
245 Market Street
San Francisco, California 94105 U.S.A.

Published Online 19 October 2016